

UC Irvine

UC Irvine Previously Published Works

Title

Augmented Antitumor Activity for Novel Dual PI3K/BDR4 Inhibitors, SF2523 and SF1126 in Ewing Sarcoma

Permalink

<https://escholarship.org/uc/item/5vm2r5rx>

Journal

Journal of Pediatric Hematology/Oncology, 43(3)

ISSN

1077-4114

Authors

Goldin, Amanda N
Singh, Alok
Joshi, Shweta
et al.

Publication Date

2021-04-01

DOI

10.1097/mpb.0000000000002054

Peer reviewed

Augmented Antitumor Activity for Novel Dual PI3K/BRD4 Inhibitors, SF2523 and SF1126 in Ewing Sarcoma

Amanda N. Goldin, MD,*† Alok Singh, PhD,† Shweta Joshi, PhD,†
Christina Jamieson, PhD,‡ and Donald L. Durden, MD, PhD†

Summary: Ewing sarcoma (ES) is the second most common pediatric bone cancer. Despite recent advances in the treatment, patients with metastatic tumors have dismal prognosis and hence novel therapies are urgently needed to combat this cancer. A recent study has shown that phosphoinositide-3 kinase (PI3K) inhibitors can synergistically increase sensitivity to bromodomain and extraterminal domain inhibitors in ES cells and therefore combined inhibition of PI3K and bromodomain and extraterminal domain bromodomain proteins might provide benefit in this cancer. Herein, we have investigated the efficacy of dual PI3K/BRD4 inhibitors, SF2523 and SF1126, for their antitumor activity in ES cell lines. The effect of SF1126 and SF2523 on cell viability and PI3K signaling was assessed on a panel of human ES cell lines. To evaluate the antitumor activity of SF1126, A673 cells were injected intraperitoneally into RAG-2^{-/-} mice and treated with 50 mg/kg SF1126 6 days per week, for 30 days. Both SF1126 and SF2523 decreased cell survival and inhibited phosphorylation of AKT in human ES cell lines. In vivo, SF1126 showed a significant reduction in tumor volume. These results suggest that dual PI3K/BRD4 inhibitor, SF1126, has antitumor activity in ES models.

Key Words: Ewing sarcoma (ES), dual inhibition, phosphoinositide-3 kinase (PI3K) pathway, bromodomain and extraterminal domain (BET) proteins, SF1126, SF2523

(*J Pediatr Hematol Oncol* 2021;00:000–000)

Ewing sarcoma (ES) is the second most common childhood and adolescent bone and soft tissue tumor, found most commonly in the pelvis and the diaphysis of long bones.^{1–5} It is an aggressive tumor, and while advances in treatment have improved the survival rate from 10% to 55%–75% for patients with no known metastases, for patients with metastatic disease the survival rate is only 15% to ~25% at 5 years.³ Furthermore, after recurrence, only 5% of patients live for > 3 years.⁶ Current therapy consists of a combination of chemotherapy, radiation, and surgery. High-dose chemotherapy can be effective but side effects are severe, including neutropenia, thrombocytopenia, and immunosuppression.^{6–8}

Phosphoinositide-3 kinase (PI3K) signaling pathway is activated downstream of several growth factor receptors and has been shown to mediate proliferation and survival signals in tumor cells.^{9,10} Activation of PI3K signaling and loss of its negative regulator, PTEN, has been reported in various cancers.¹⁰ Dysregulation of PTEN/PI3K signaling axis has also been reported in a variety of ES cell lines and in tumor tissues at diagnosis.^{5,11,12} In fact, roughly 25% of ES tumors have been suggested to show loss of tumor suppressor, *PTEN* gene.¹¹ A previous report has shown that PI3K inhibitors have shown benefit in suppressing ES cell growth.⁴ Despite the evidence that PI3K plays a significant role in the growth of ES there are currently no drugs available that target this pathway in this disease.

Bromodomain and extraterminal domain (BET) proteins, including BRD2, BRD3, BRD4, and BRDT, are chromatin regulatory proteins and regulate transcription of many important genes and are associated with cancer progression.¹³ BRD4 is known to propagate the cell cycle and activate the *cMYC* oncogene.^{14,15} Recently, inhibition of the BET proteins has been associated with decreased expression of the oncogenic EWS/FLI-1 fusion protein that present in nearly all ESs.^{14,16} There are no reports examining the role of BET bromodomain inhibitors in ES pathogenesis.

Previous studies have commented on the benefits of dual inhibition in utilization of the PI3K and BET bromodomain pathways.^{17–21} SF1126 is the first PI3K and BET bromodomain dual inhibitor which has shown potent antitumor activity in various cancer models.^{20,22–26} It is a prodrug of the compound SF1101 (also known as LY294002), which was not a drug candidate because of insolubility and a short half-life, however, it was the first PI3K inhibitor shown to have antitumor activity in vivo.¹⁸ To achieve ideal pharmacological properties, the active PI3K site was linked to an RGDS peptide as SF1126 for targeting the $\alpha\beta3$ integrin of tumor and tumor microenvironment cells, including endothelial cells and macrophages.^{23,27} The BET bromodomain inhibitory activity of SF1101 was shown recently by Dittmann et al,²⁴ and the Darden laboratory was able to replicate and confirm that SF1126 blocks BRD4 binding to the MYCN promoter (Fig. 1). SF1126 has been shown to inhibit MYCN and *cMYC*, which are proteins suggested to be involved in ES.^{17,20,28,29} Furthermore, it has been shown that combined inhibition of BET proteins and PI3K signaling can help prevent drug resistance in ES³⁰; SF1126 is the first drug which can hit both signaling proteins. The drug has been through phase I trials in adults, and showed general suppression of disease with limited side effects, including one grade III and no grade IV dose-limiting toxicity events.^{22,31} SF2523 is another novel dual PI3K and BET inhibitor generated in Darden lab that is more potent than SF1126, and has shown to be effective in a variety of cancers.^{19,21,27,32,33} SF2523P is a single BET inhibitor with a similar potency to SF2523. The goal of the authors in this study included showing the efficacy of a

Received for publication April 3, 2020; accepted December 3, 2020.
From the *Department of Orthopedic Surgery; †Department of Pediatrics, Division of Pediatric Hematology-Oncology, UCSD Rady's Children's Hospital; and ‡Department of Urology, Moore's Cancer Center, University of California San Diego, San Diego, CA.
D.L.D. has a significant financial conflict of interest with SignalRx Pharmaceuticals as he is a founder, a board member, and a member of the scientific advisory board. This relationship has been disclosed and reviewed by the conflict of interest committee at the University of California San Diego. The remaining authors declare no conflict of interest.
Reprints: Donald L. Durden, MD, PhD, 3010 Children's Way, San Diego, CA 92123 (e-mail: ddurden@health.ucsd.edu).
Copyright © 2021 Wolters Kluwer Health, Inc. All rights reserved.

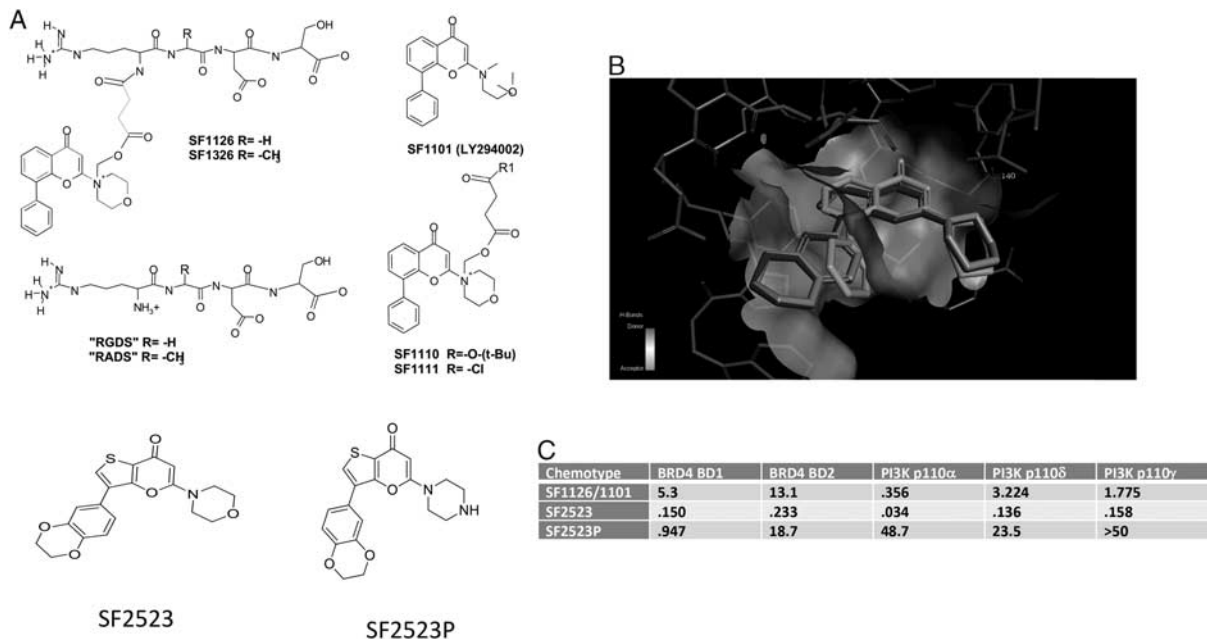


FIGURE 1. Dual PI3K/BRD4 inhibitors, SF1126, SF2523, and SF2523P. A, Structure of SF1126, SF2523, and SF2523P. B, BRD4-BD1 (PDB ID: 4CFK) co-crystallized with LY294002, SF2523 (docked) and SF2523P (docked) Hydrogen bond between the carbonyl group of LY294002 and amide group of Asn140 shown in green dotted lines. C, Table of IC₅₀ values (μM concentrations) for 3 chemotypes against targets PI3K and BRD4. PI3K indicates phosphoinositide-3 kinase.

dual PI3K/BET inhibitor in ES, including SF1126 and SF2523, in contrast with a single inhibitor, such as SF2523P.

MATERIALS AND METHODS

Tissue Culture, Cell Lines, and Reagents

A673, EWS502, SK-N-MC, SK-PN-DW, and RDES human cell lines were obtained from the ATCC collection and provided by Sun Choo, M.D., UC San Diego Department of Pediatrics. Cells were maintained in DMEM+10% FBS+100 μg/mL streptomycin+100 units/mL penicillin. All cell lines were authenticated by short tandem repeat DNA profiling before being received by Sun Choo lab. For Western blot experiments, antibodies specific for AKT, pAKT^{S473}, and EWS were obtained from Cell Signaling Technologies (Danvers, MA), and actin primary antibodies were obtained from Santa Cruz (Dallas, TX). SF1126, SF2523, and SF2523P were obtained from SignalRx Pharmaceuticals (San Diego, CA).

Cell Viability Assays

Cells at the concentration of $5 \times 10^3/100 \mu\text{L}$ were added in triplicate to a 96-well plate. Cells were cultured for 24 hours followed by treatment with SF1126, SF2523, or SF2523P. After 48 hours, AlamarBlue (Thermo Fisher Scientific, Waltham, MA) was added and plates were incubated at 37°C in 5% CO₂ for 3 hours. Fluorescence signals were read as emission at 590 nm after excitation at 560 nm.

Western Blot Analysis

Cells were plated in 10 cm tissue culture dishes and were treated with varying concentrations of SF1126 (5, 15, and 25 μM) and SF2523 and SF2523P (0.1, 1, and 5 μM). After 30 minutes, the cells were lysed with RIPA lysis buffer (Thermo Fisher Scientific) and proteins were quantitated by

the BCA protein assay (Thermo Fisher Scientific). Equal amounts of protein were resolved by polyacrylamide gels, transferred to nitrocellulose membranes, and probed with p-AKT, AKT, EWS, and actin primary antibodies (Cell Signaling Technologies). ImageJ 1.49v software was used to calculate densitometry data.

In Vivo Studies

Recombination Activation Gene-2-deficient (RAG-2) mice were a gift from Christina Jamieson, PhD (University of California San Diego). Mice were maintained in the Moores Cancer Center vivarium at University of California San Diego. All experiments were performed using procedures approved by the University of California San Diego IACUC committee. For in vivo experiments, A673 cells were stably transfected with a plasmid encoding the *luciferase* and *mCherry* gene expression. 5×10^4 *luciferase* positive A673 cells in 15 μL media were mixed with 15 μL of matrigel. The cells were injected as previously described by Vormoor and colleagues, and similarly to the process described by Sasaki et al and colleagues, yet in a more quick and less invasive manner.^{34,35} The mice were first anesthetized with 60 mg/kg ketamine (Fort Dodge Animal Health, Overland Park, KS) and 20mg/kg xylazine (Ben Venue Laboratories, Bedford, OH). For each mouse, the right hind leg was shaved, and the knee was hyper-flexed. A 25 G needle was used to puncture through the patella and between the condyles of the femur, into the intramedullary canal of the femur. Using the needle, the outer cortex was palpated to ensure correct position inside the canal. The 25 G needle was removed and an insulin needle and syringe with the 30 μL solution of 50,000 cells, media, and matrigel was inserted, and injected into the intramedullary canal. Afterwards, the needle was removed, and a bacitracin gel was placed on the injection site. This was repeated for a total

of 10 mice for each experiment, for a total of 2 experiments. Mice were monitored until they regained consciousness. Three days after the intrafemoral injections, the IVIS Spectrum in vivo imaging system (PerkinElmer, Waltham, MA) was used to detect and quantitate the luciferase expressing cells growing in each of our 10 mice. At that time mice were then randomly placed into 2 groups, and SF1126 at a dose of 50 mg/kg was injected subcutaneously in and around the right hind leg 6 days a week, versus a control group treated with daily subcutaneous injections of 100 μ L of phosphate-buffered saline. The trial was conducted over a total of 30 days. Tumor size was monitored through the IVIS system weekly, and with caliper measurements every 3 days, once the tumors had grown to be externally visible. After 30 days the mice were euthanized. Tumors, including the involved femur and its visible soft tissue mass, were marginally excised with standard surgical technique and weighed at that time.

Tumor Tissue Analysis

Tissue collected from tumor specimens was stored at -80°C and used for Western blot analysis. Remaining tumor and leg specimens were fixed in formalin. Micro computed tomography (m-CT) analysis was conducted on these specimens.

Statistical Analysis

The Student *t* test was used to evaluate the differences between groups of drug-treated mice to vehicle-treated controls.

RESULTS

Dose-Dependent Effects of SF1126, SF2523, and SF2523P on ES Cells in vitro

On the basis of previous reports suggesting the role of PI3K signaling in the progression of ES tumors,^{5,11} we analyzed the efficacy of our dual PI3K/BRD4 inhibitors, SF1126, SF2523, SF2523P in decreasing cell viability in A673, EWS502, SK-N-MC, SK-PN-DW, and RDES cell lines. Our results suggest that the drug is effective in suppressing cell survival in a dose-dependent manner in 4 of the 5 cell lines (Fig. 2A). For SF1126, logarithmic dose-response curves showed an IC_{50} of 6.7 μM for A673, 13.9 μM for EWS502, 11.4 μM for SK-N-MC and 13.4 μM for SK-PN-DW. For SF2523, logarithmic dose-response curves showed an IC_{50} of 3.5 μM for A673, 5.9 μM for EWS502, 3.8 μM for SK-N-MC, and 6.2 μM for SK-PN-DW. For SF2523P, logarithmic dose-response curves showed an IC_{50} of 33.5 μM for A673, 38.1 μM for EWS502, 14.6 μM for SK-N-MC, and 22.3 μM for SK-PN-DW. Only the RDES cell line did not show a dose-dependent response to SF1126, SF2523, and SF2523P.

PI3K/BRD4 Dual Inhibitors Inhibit Phosphorylation of AKT in a Dose-dependent Manner

A673, EWS502, SK-N-MC, SK-PN-DW, and RDES cell lines treated with various concentrations of SF1126 showed a dose-dependent decrease in levels of p-AKT. The decrease in the expression of EWS protein was not significant (Fig. 2B). Furthermore, A673, EWS502, SK-N-MC, and SK-PN-DW cell lines treated with different doses of SF2523 also showed decrease in phosphorylation of AKT at lower concentration of SF2523. At higher doses of SF2523 we observed a decrease in protein expression of EWS in the A673 cell line (Fig. 2C). Treatment of ES cells

with SF2523P did not show a decrease in p-AKT levels, however, there was a decrease in EWS in the A673 cell line (Fig. 2D).

An Intrafemoral Injection of A673 Cells is an Efficient and Quick Method of Creating a Mouse Xenograft

The 5×10^4 A673 cells that were injected into the medullary canal of the femurs grew quickly in the RAG-2-deficient mice. The mice showed a photon signal through luciferase and the IVIS Spectrum in vivo imaging system 3 days after injection. Comparably, a mouse with 50,000 cells injected into the flank did not show a signal on the IVIS for 30 days.

SF1126 Causes a Slowing of Tumor Growth Rate of A673 Cells In Vivo

The IVIS Spectrum in vivo imaging system demonstrated a significant difference in photon emission between the SF1126 and vehicle control treated mice (Fig. 3A). By day 23 of the experiment the difference was significant with a *P* value of <0.01 , and a *P* value of 0.03 on day 29 (Fig. 3B). Caliper measurements allowed the measuring of tumor volume over the course of the drug trial. Results were also significant as of day 23, with a *P* value of 0.02, followed by a *P* value of 0.03 on day 26, and a *P* value of <0.01 on days 29 and 30 (Fig. 3C). The drug trial was repeated, and significant results were confirmed. In the second experiment there was a significant difference in photon emission between the groups on day 30 ($P < 0.01$) and a difference in tumor caliper on day 27 and 30 ($P = 0.03$ and 0.02, respectively). In the first experiment 1 mouse in the treatment group died of an unidentified cause midway through the drug trial. Throughout the experiment there were no significant differences in mouse weights in the 2 groups. The only obvious side effect of the drug was some skin ulceration at the injection site.

SF1126 is Effective at Decreasing p-AKT and EWS Quantities In Vivo

Homogenized tissue from the mouse tumors that was analyzed for expression of p-AKT and EWS showed a decrease phosphorylation of AKT and expression of EWS in the treatment group versus the control group, and this was numerically quantified with ImageJ software (Fig. 3D). Calculating the p-AKT:AKT ratio, there was a mean ratio of 0.86:1 in the SF1126 treated mice, versus 2.44:1 in the control mice. This was significant, with a *P* value of 0.02. The EWS:tubulin ratio showed a mean ratio of 1.3:1 (± 0.08) in the SF1126 treated mice, versus 1.5:1 (± 0.04) in the control mice. This proved to be significant as well, with a *P* value of 0.02 (Fig. 3E).

SF1126 Decreases Bony Destruction in Mice Compared With Control

Micro-CT analysis conducted on all tumor-side hind legs of mice after necropsy showed a lesser amount of periosteal reaction and destruction of bone in the SF1126 mice versus the control group (Fig. 3F). This was qualitatively demonstrated throughout the diaphysis of the bones.

DISCUSSION

The previously reported synthetic lethality between PI3K and BRD4 in different cancers including ES has led us to design in silico our potent dual PI3K/BRD4 inhibitory

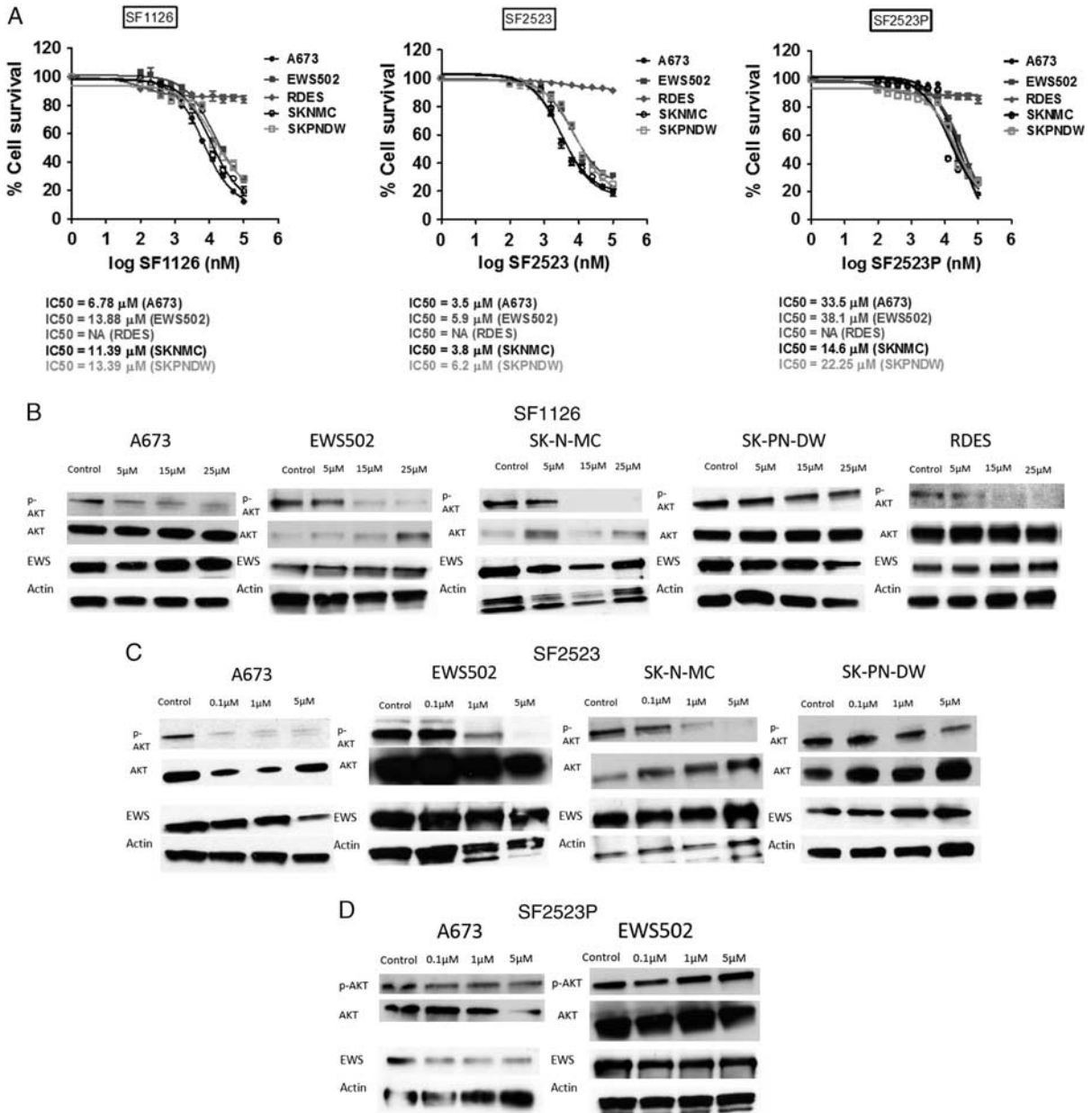


FIGURE 2. SF1126 and SF2523 decreases cell viability and phosphorylation of AKT in Ewing sarcoma cell lines. A, IC₅₀ curves of the 5 ES cell lines treated with SF1126, SF2523, and SF2523P. B, WB results for A673, EWS502, SK-N-MC, SK-PN-DW, and RDES treated with different concentrations of SF1126 followed by lysate preparation after 30 minutes of treatment and Western blot analysis. C, WB results for A673, EWS502, SK-N-MC, and SK-PN, DW treated with various doses of SF2523 for 30 minutes followed by lysate preparation and western blot. D, WB results for A673 and EWS502 with 30 minutes of SF2523P treatment at 0.1, 1, and 5 μM concentrations. WB indicates western blot.

chemotypes, SF2523 and SF2523P (no PI3K inhibitory property). This was in an effort to test the effects of dual versus single chemotypic inhibition of ES survival.^{17,19} SF1126 and SF2523 have potent PI3K/BRD4 inhibitory activity, and previous studies have confirmed the simultaneous blockage of PI3K/BRD4 pathways, suggesting that these pathways are an effective therapeutic target in ES.^{15,17,19,20} Previous studies that have compared dual inhibition of PI3K/BRD4 to solely PI3K or BRD4 have found increased cell death at lower drug potencies with the

dual inhibitors. This has been appreciated when comparing the dual inhibitors SF1126, SF2523, and LY294002 with the single PI3K inhibitors BEZ-235, BKM120, Cal101, and Wortmannin, and the single BRD4 inhibitors JQ1 and LY303511.^{15,17,19} Importantly, this is the first study to specifically compare a dual inhibitor (SF2523) to its identical in silico engineered piperazine derivative single inhibitor (SF2523P). In this experiment, the 2 different compounds had different IC₅₀ values for the ES cell lines, ranging 3.5 to 6.2 μM for SF2523 and 14.6 to 38.1 μM for SF2523P. This

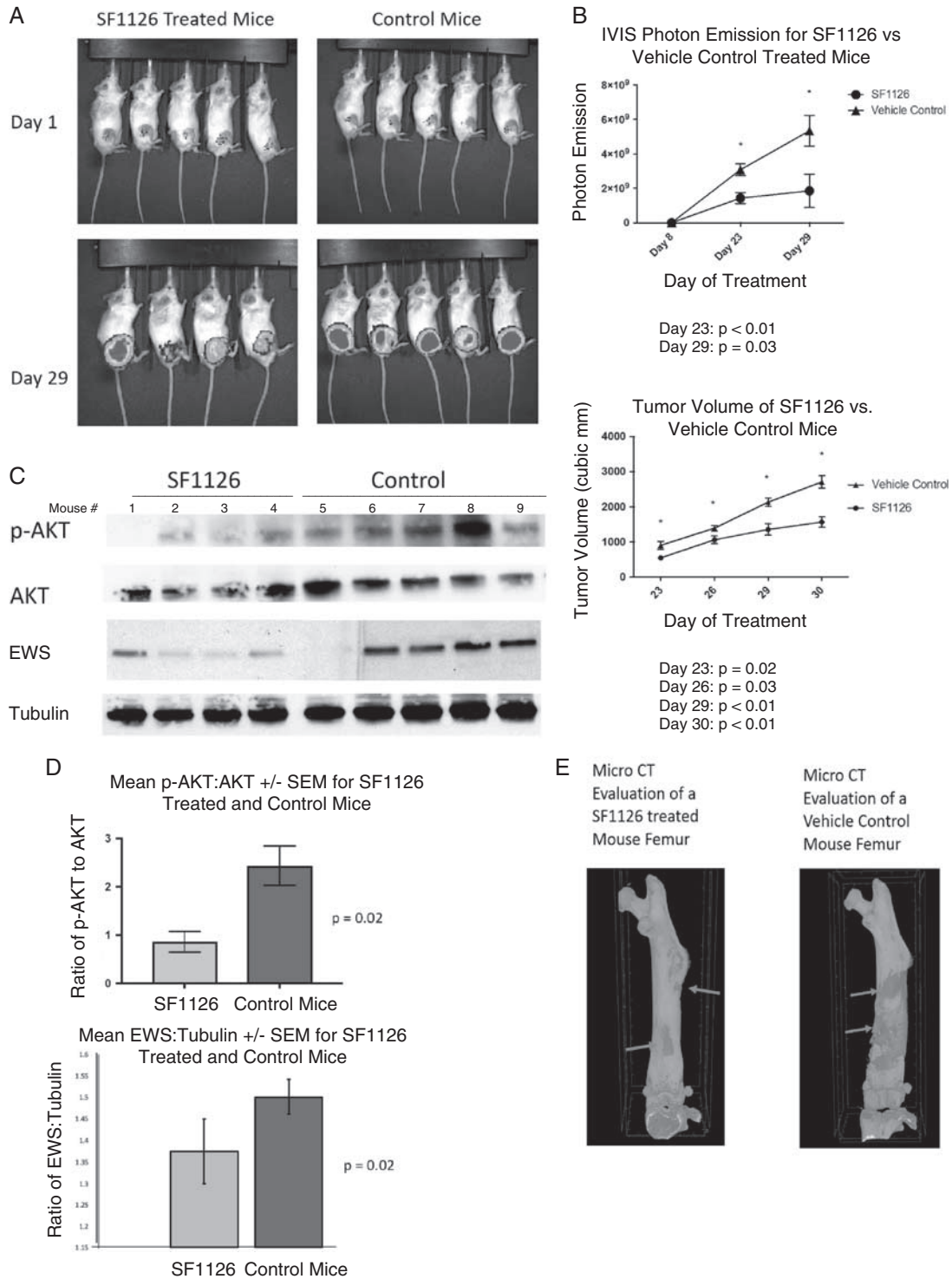


FIGURE 3. SF1126 reduces tumor growth in Ewing sarcoma model. A, IVIS in vivo imaging results of the RAG-2 mice treated with SF1126 versus vehicle control (phosphate-buffered saline). Dark color indicates a higher photon density, which indicates greater mass and biological activity of the tumor. B, Graphical demonstration of the difference in photon emission and tumor volume of the treatment versus control groups in 2 experiments. C, WB results for homogenized tumor tissue from mice treated with drug (left) and vehicle control (right). There are decreased quantities of p-AKT and EWS in the SF1126 treated mice than the control group. D, Graphical demonstration of densitometry data from western blots. E, Micro-CT scans of treatment versus control mouse femurs. CT indicates computed tomography; RAG-2, Recombination Activation Gene-2; WB, western blot.

demonstrates the influence of dual inhibition and PI3K targeting in limiting cell growth and survival in ES systems.

Previously, LY294002 and SF1126 has been shown to cause cell cycle arrest and to induce apoptosis in a hepatocellular carcinoma model.²⁰ To the best of our knowledge, SF1126 has not been tested on ES previously. Our results suggest IC₅₀'s ranging from 6.7 μM (A673) to 13.9 μM (EWS502) for SF1126. This is similar to previous dose-response results with SF1126, such as multiple myeloma, of which cell lines showed IC₅₀'s of 8.9 μM to 11.9 μM.³⁶ SF2523 has been shown to be a potent dual PI3K/BET bromodomain inhibitor, which has never been tested on ES cells.¹⁹ The IC₅₀ values of the drug ranged from 3.5 μM (A673) to 6.2 μM (SK-PN-DW). With such small micromolar quantities, it is possible that this drug could have great effect on ES, while being well tolerated in its small dosages. SF2523P was designed to have the same potency as SF2523; however, it is a single inhibitor of BET/bromodomain proteins. Therefore, the IC₅₀ values for SF2523P are higher as expected, ranging from 14.6 μM (SK-N-MC) to 38.1 μM (EWS502), again signifying the increased efficacy of a dual inhibitor versus a single inhibitor. Finally, it should be noted that out of the 5 cell lines, a dose-dependent inhibition of RDES with SF1126, SF2523, or SF2523P was not observed. While RDES has shown up in the literature as a tested cell line of ES, specific information about the cell line's nature could not be found.³⁷ Subjectively, the RDES cell line was the most difficult to culture, growing at a rate several times slower than the other cell lines. The cells also appeared spherical in appearance, while the other cell lines grew in a branching formation. Our hypothesis is that RDES cells have low baseline PI3K/BET bromodomain activity, which is why inhibition does not show a dose-dependent decrease in cell survival; however, this was beyond the scope of the current study. Further experiments need to be conducted to find the cause of this finding.

Western blot results showed a dose-dependent downregulation of p-AKT in vitro, and p-AKT downregulation in association with a decrease in rate of tumor growth after treatment of ES cells with dual PI3K/BET bromodomain inhibitors in vivo. These results were expected, as the literature has shown the PI3K pathway to have an active role in ES. However, it should be noted that in some of the AKT blots there was some over exposure, which could underestimate the denominator in the p-AKT to AKT ratio. Increased amounts of PIK3R3 and decreased amounts of PTEN have been seen in a variety of Ewing cell lines,^{5,11,12} and ES cell population growth can be decreased by suppression of the PI3K pathway through suppression of the *PIK3CD* gene.⁴ All 5 cell lines showed a downregulation of p-AKT after SF1126 treatment, including the RDES cell line, which did not show a dose-response relationship in the survival curve drug assays. This further supports the hypothesis that RDES is sensitive to the drug but has low baseline levels of PI3K activity. The downregulation of p-AKT was demonstrated with A673 and SF1126 in the in vivo experiments. LY294002 has previously shown to decrease p-AKT levels in ES cells.³⁸

Western blot results showed a decrease in EWS expression after treatment of ES cells with the drugs SF1126, SF2523, and SF2523P. The difference in the in vivo EWS expression was striking, however, it must be noted that there was some overexposure of actin and tubulin in both the in vitro and in vivo studies, which

could have an effect on the overall EWS to control ratio. In regard to the densitometry data, it should be noted that control mouse #5 had an abnormally low quantity of EWS for unknown reasons. Despite this, the difference in in vivo EWS quantity still proved to be significant. Interestingly, in the in vitro Western blot studies there was decrease in EWS with SF2523P. This suggests that BET bromodomain inhibition has a role to directly decrease EWS expression. The importance of BET bromodomain inhibition, and particularly BRD4, has been previously shown through the use of JQ1.¹⁶ PI3K inhibition has also been demonstrated to have an effect in decreasing EWS.³⁷ To the writers' knowledge, this is the first demonstration of a dual PI3K/BET bromodomain inhibitor showing a decrease in EWS, and our results suggest utility of such a dual inhibitor in the management of the protein's expression.

A 25% of ES tumors have been suggested to have a reduced quantity of PTEN.¹¹ The EWS502 cell line is completely void of PTEN, while PTEN is expressed in the A673, SK-PN-DW, SK-N-MC, and RDES cell lines.^{5,11,12} The EWS502 cell line was found to have higher IC₅₀ values with all three inhibitors, likely because of its deletion mutation of *PTEN*. The knowledge that a lack of PTEN requires higher quantities of inhibitor is important as clinicians go forth in using these drugs with patients. Patients who have a *PTEN* mutation will likely either require higher quantities of drug (increasing their risk of toxicity,) or will not respond to the drug at all.

The intrafemoral injection of luciferase transfected ES cells has proved to be an effective method for creating a xenograft that more closely parallels the pathology seen in human ES. The method can be performed in <15 minutes per mouse.³⁵ This method is simpler than that described by Sasaki et al,³⁴ which requires a surgical procedure and sophisticated surgical tools. The vast majority of the ES xenografts found in the literature are created by a subcutaneous injection either over the leg or over the flank.^{3,14,39} While this method is fast and easy, it does not create a diaphyseal tumor (which is classically seen in human ES); furthermore, the tumors grow more slowly than the tumors in the current experiment, which were apparent by IVIS just 3 days after injection of A673 cells.^{1,39}

The current study shows that the drug SF1126 is effective at slowing the rate of tumor growth in A673 cells in vivo. This is the first in vivo study that has been conducted with SF1126 and ES. Monitoring tumor size by photon intensity through the IVIS system and by caliper measurements, a significant difference was shown in rates of tumor growth and size. The experiment was repeated, and the results were again significant. This is noteworthy, as SF1126 is already in phase I clinical trials in children with neuroblastoma and has passed phase I trials in adults; therefore, it is reasonable to consider testing the drug in children with sarcomas, as it has shown to be effective in an animal model.²² However, testing further with multiple cell lines in vivo would provide more data regarding the efficacy of the dual inhibitor in ES, and may be considered before proceeding with actual ES patients. It is probable that the drug would have a synergistic effect with other chemotherapy drugs used for ES.¹⁸ More research and animal studies are needed to explore this hypothesis.

Micro-CT scans were conducted on the hind legs of the mice after necropsy and qualitatively demonstrated increased periosteal reaction and superficial bony lesions on the control group than the treatment group. This is similar to the classic

“onion skin” periosteal reactions humans with ES develop.^{11,40,41} The relationship between periosteal reactions and pain is well known, and a study by Mach and colleagues showed that the periosteum had the highest density of sensory nerve fibers than any other part of the bone.^{42,43} A literature search did not reveal any studies that look into whether a decrease in periosteal reaction leads to a decrease in bone pain in ES. Considering the immense number of sensory nerve fibers on the periosteum it is probable that SF1126 would have a bone pain limiting effect. More studies are needed to determine the exact relationship between pain, the periosteum, and SF1126, as well as to quantify the exactly amount of periosteal involvement.

In summary, the current study demonstrates the effectiveness of PI3K/BET bromodomain inhibitors in reducing tumor growth in ES, as well as the utility of a dual inhibitor over a single inhibitor. This efficacy is demonstrated in vivo and in vitro. Given the efficacy of the drug in the current study, and the positive results the well-tolerated SF1126 has shown thus far in clinical trials, its use in patients with sarcomas should be considered.

ACKNOWLEDGMENTS

Aided by a grant from the Orthopaedic Research and Education Foundation with funding provided by Exachtech awarded to ANG, and grants CA215656 from NIH awarded to DLD. Thank you to Michael Alcaraz, Adam Burgoyne, Mima Zulcic, and Michelle Muldong for laboratory assistance, Esther Cory and Koichi Masuda for assistance with CT imaging, and Sun Choo for providing cell lines of Ewing Sarcoma.

REFERENCES

- McKinsey EL, Parrish JK, Irwin AE, et al. A novel oncogenic mechanism in Ewing sarcoma involving IGF pathway targeting by EWS/Fli1-regulated microRNAs. *Oncogene*. 2011;30:4910–4920.
- Kamura S, Matsumoto Y, Fukushi J-I, et al. Basic fibroblast growth factor in the bone microenvironment enhances cell motility and invasion of Ewing's sarcoma family of tumours by activating the FGFR1-PI3K-Rac1 pathway. *Br J Cancer*. 2010;103:370–381.
- Mendoza-Naranjo A, El-Naggar A, Wai DH, et al. ERBB4 confers metastatic capacity in Ewing sarcoma. *EMBO Mol Med*. 2013;5:1019–1034.
- Li J, You T, Jing J. MiR-125b inhibits cell biological progression of Ewing's sarcoma by suppressing the PI3K/Akt signalling pathway. *Cell Prolif*. 2014;47:152–160.
- Niemeyer BF, Parrish JK, Spoelstra NS, et al. Variable expression of PIK3R3 and PTEN in Ewing Sarcoma impacts oncogenic phenotypes. *PLoS One*. 2015;10:1–14.
- Meyers PA. Systemic therapy for osteosarcoma and Ewing sarcoma. *Am Soc Clin Oncol Educ B*. 2015;35:e644–e647.
- Loschi S, Dufour C, Oberlin O, et al. Tandem high-dose chemotherapy strategy as first-line treatment of primary disseminated multifocal Ewing sarcomas in children, adolescents and young adults. *Bone Marrow Transplant*. 2015;50:1083–1088.
- Paioli A, Luksch R, Fagioli F, et al. Chemotherapy-related toxicity in patients with non-metastatic Ewing sarcoma: influence of sex and age. *J Chemother*. 2014;26:49–56.
- Liu P, Cheng H, Roberts TM, et al. Targeting the phosphoinositide 3-kinase pathway in cancer. *Nat Rev Drug Discov*. 2009;8:627–644.
- Chalhoub N, Baker SJ. PTEN and the PI3-kinase pathway in cancer. *Annu Rev Pathol Mech Dis*. 2009;4:127–150.
- Moore DD, Haydon RC. Ewing's sarcoma of bone. *Cancer Treat Res*. 2014;162:93–115.
- Patel M, Gomez NC, Mcfadden AW, et al. PTEN deficiency mediates a reciprocal response to IGFI and mTOR inhibition. *Mol Cancer Res*. 2014;473:1610–1620.
- Stathis A, Bertoni F. BET proteins as targets for anticancer treatment. *Cancer Discov*. 2018;8:24–36.
- Jacques C, Lamoureux F, Baud M, et al. Targeting the epigenetic readers in Ewing sarcoma inhibits the oncogenic transcription factor EWS/Fli1. *Oncotarget*. 2016;7:24125–24140.
- Zhu H, Mao J, Wang Y, et al. Dual inhibition of BRD4 and PI3K-AKT by SF2523 suppresses human renal cell carcinoma cell growth. *Oncotarget*. 2017;8:98471–98481.
- Hensel T, Giorgi C, Schmidt O, et al. Targeting the EWS-ETS transcriptional program by BET bromodomain inhibition in Ewing sarcoma. *Oncotarget*. 2015;5:1451–1463.
- Erdreich-Epstein A, Singh AR, Joshi S, et al. Association of high microvessel $\alpha\beta 3$ and low PTEN with poor outcome in stage 3 neuroblastoma: rationale for using first in class dual PI3K/BRD4 inhibitor, SF1126. *Oncotarget*. 2017;8:52193–52210.
- Peirce SK, Findley HW, Prince C, et al. The PI-3 kinase-Akt-MDM2-survivin signaling axis in high-risk neuroblastoma: a target for PI-3 kinase inhibitor intervention. *Cancer Chemother Pharmacol*. 2011;68:325–335.
- Andrews FH, Singh AR, Joshi S, et al. Dual-activity PI3K-BRD4 inhibitor for the orthogonal inhibition of MYC to block tumor growth and metastasis. *Proc Natl Acad Sci U S A*. 2017;114:E1072–E1080.
- Singh AR, Joshi S, Burgoyne AM, et al. Single agent and synergistic activity of the “first-in-class” dual PI3K/BRD4 inhibitor SF1126 with sorafenib in hepatocellular carcinoma. *Mol Cancer Ther*. 2016;15:2553–2562.
- Joshi S, Singh AR, Liu KX, et al. SF2523: Dual PI3K/BRD4 inhibitor blocks tumor immunosuppression and promotes adaptive immune responses in cancer. *Mol Cancer Ther*. 2019;18:1036–1044.
- Mahadevan D, Chiorean EG, Harris WB, et al. Phase I pharmacokinetic and pharmacodynamic study of the pan-PI3K/mTORC vascular targeted pro-drug SF1126 in patients with advanced solid tumours and B-cell malignancies. *Eur J Cancer*. 2012;48:3319–3327.
- Garlich JR, De P, Dey N, et al. A vascular targeted pan phosphoinositide 3-kinase inhibitor prodrug, SF1126, with antitumor and antiangiogenic activity. *Cancer Res*. 2008;68:206–215.
- Dittmann A, Werner T, Chung CW, et al. The commonly used PI3-kinase probe LY294002 is an inhibitor of BET bromodomains. *ACS Chem Biol*. 2014;9:495–502.
- Joshi S, Singh AR, Durden DL. Pan-PI-3 kinase inhibitor SF1126 shows antitumor and antiangiogenic activity in renal cell carcinoma. *Cancer Chemother Pharmacol*. 2015;75:595–608.
- Singh AR, Joshi S, George E, et al. Anti-tumor effect of a novel PI3-kinase inhibitor, SF1126, in (12) V-Ha-Ras transgenic mouse glioma model. *Cancer Cell Int*. 2014;14:1–12.
- Joshi S, Singh AR, Zulcic M, et al. A macrophage-dominant PI3K isoform controls hypoxia-induced HIF1 α and HIF2 α stability and tumor growth, angiogenesis, and metastasis. *Mol Cancer Res*. 2014;12:1520–1531.
- Ambati SR, Lopes EC, Kosugi K, et al. Pre-clinical efficacy of PU-H71, a novel HSP90 inhibitor, alone and in combination with bortezomib in Ewing sarcoma. *Mol Oncol*. 2014;8:323–336.
- Stratikopoulos EE, Dendy M, Szabolcs M, et al. Kinase and BET inhibitors together clamp inhibition of PI3K signaling and overcome resistance to therapy. *Cancer Cell*. 2015;27:837–851.
- Loganathan SN, Tang N, Holler AE, et al. Targeting the IGF1R/PI3K/AKT pathway sensitizes ewing sarcoma to BET bromodomain inhibitors. *Mol Cancer Ther*. 2019;18:929–936.
- Su JD, Mayo LD, Donner DB, et al. PTEN and phosphatidylinositol 3'-kinase inhibitors up-regulate p53 and block tumor-induced angiogenesis: evidence for an effect on the tumor and endothelial compartment. *Cancer Res*. 2003;63:3585–3592.
- Singh AR, Joshi S, Garlich JR, et al. Abstract A27: dual PI3K/BRD4 (kinase/epigenetic) inhibitors for maximal MYC control in cancer therapeutics. *Mol Cancer Ther*. 2015;14:A27.

33. Morales GA, Garlich JR, Su J, et al. Synthesis and cancer stem cell-based activity of substituted 5-morpholino-7H-thieno[3,2-b]pyran-7-ones designed as next generation PI3K inhibitors. *J Med Chem*. 2013;56:1922–1939.
34. Sasaki H, Iyer SV, Sasaki K, et al. An improved intrafemoral injection with minimized leakage as an orthotopic mouse model of osteosarcoma. *Anal Biochem*. 2015;486:70–74.
35. Vormoor B, Knizia HK, Batey MA, et al. Development of a preclinical orthotopic xenograft model of Ewing sarcoma and other human malignant bone disease using advanced in vivo imaging. *PLoS One*. 2014;9:1–14.
36. De P, Dey N, Terakedis B, et al. An integrin-targeted, pan-isoform, phosphoinositide-3 kinase inhibitor, SF1126, has activity against multiple myeloma in vivo. *Cancer Chemother Pharmacol*. 2013;71:867–881.
37. Giorgi C, Boro A, Rechfeld F, et al. PI3K/AKT signaling modulates transcriptional expression of EWS/FLI1 through specificity protein 1. *Oncotarget*. 2015;6:28895–28910.
38. Kilic-eren M, Boylu T, Tabor V. Targeting PI3K/Akt represses Hypoxia inducible factor-1 α activation and sensitizes Rhabdomyosarcoma and Ewing's sarcoma cells for apoptosis. *Cancer Cell Int*. 2013;13:1–8.
39. Dalal S, Burchill SA. Preclinical evaluation of vascular-disrupting agents in Ewing's sarcoma family of tumours. *Eur J Cancer*. 2009;45:713–722.
40. Wenaden AET, Szyszko TA, Saifuddin A. Imaging of periosteal reactions associated with focal lesions of bone. *Clin Radiol*. 2005;60:439–456.
41. Iwamoto Y. Diagnosis and treatment of Ewing Sarcoma. *Japan J Clinial Oncol*. 2007;37:79–89.
42. Rana RS, Wu JS, Eisenberg RL. Periosteal reaction. *AJR Am J Roentgenol*. 2009;259–272.
43. Mach DB, Rogers SD, Sabino MC, et al. Origins of skeletal pain: sensory and sympathetic innervation of the mouse femur. *Neuroscience*. 2002;113:155–166.